OMAE2017-62030

Drag On Nets Fouled with Blue Mussel (*Mytilus Edulis)* and Sugar Kelp (*Saccharina Latissima*) and Parameterization of Fouling

Lars C. Gansel
SINTEF Fisheries and Aquaculture
NTNU
Ålesund, Norway

Per Christian Endresen
SINTEF Fisheries and Aquaculture
Trondheim, Norway

Kristine Braaten Steinhovden
SINTEF Fisheries and Aquaculture
Trondheim, Norway

Stine Wiborg Dahle
SINTEF Fisheries and
Aquaculture
Trondheim, Norway

Eirik Svendsen
SINTEF Fisheries and
Aquaculture
Trondheim, Norway

Silje Forbord
SINTEF Fisheries and
Aquaculture
Trondheim, Norway

Østen Jensen
Statoil
Stjørdal, Norway

ABSTRACT

Biofouling is a serious problem in marine finfish aquaculture with a number of negative impacts. Marine growth obstructs net openings, thereby reducing water exchange through the net and affecting fish welfare and health, as well as the spreading of dissolved nutrients, particles and pathogens. Furthermore, additional water blockage leads to increased hydrodynamic forces on fish cages, which potentially threaten the structural integrity of the fish farm. However, detailed knowledge about the effects of biofouling on the flow past, and the resulting forces on fish cages, is limited and systematic investigations of the effects of different types of fouling have been called for.

This study investigates the effects of different amounts and sizes of two important fouling organisms in Norwegian aquaculture, blue mussel (*Mytilus edulis*) and kelp (*Saccharina latissima*) on the drag on net panels. Drag forces on a number of clean and fouled nets were measured in a flume tank at a flow speed of 0.1 m/s. Net solidity was calculated from images acquired of all nets in the current. The relationship between net solidity and drag was then found for clean nets and for each type of fouling, and biofouling was parameterized by comparing clean and fouled net results: for a given fouled net, a clean net can be found that experiences the same drag. The latter can then be used in numerical models to estimate the effect of fouling on net drag. That means existing models can be used to model the drag effect of fouling. This study found a solidity increase due to mussel and kelp fouling to affect drag roughly at the same rate as an increase in clean net solidity at a flow speed of 0.1 ms^{-1} and within the tested fouling size range for two net types. Therefore, existing models, describing the relationship between net solidity and drag, can be used directly or with minor alterations (especially at high solidities) to estimate effects of additional mussel and kelp fouling on drag. In contrast, wet weight seems to be unsuitable as a measure to estimate drag on nets fouled with seaweed or mussels. It should be noted that these findings are only valid under similar conditions, and that other fouling types and sizes, as well as test parameters and tank size can affect the relationship between solidity and drag.

INTRODUCTION

Marine biofouling, the undesirable accumulation of organisms on submerged surfaces, has a number of adverse effects in marine aquaculture, including reduced water exchange across nets and increased net drag [1-4]. Shortly after submergence of nets fouling organisms settle on the surface, and, given suitable conditions, both mobile and sessile biofouling can then build up very fast. Several studies report a wet weight increase of biofouling organisms on aquaculture nets within the range of kilograms per m^2 within few weeks (e.g. [5-7]) and one m^2 of net can hold up to several 10 kg of biofouling wet weight [5]. The accumulation of fouling organisms is generally associated with the occlusion of net apertures, and several studies found rates of net aperture occlusion in accordance with rapid wet weight increase. For example, [8] found a net aperture occlusion of about 20 % within only two weeks in the sea in Clift sound, Shetland, and [9] report mesh occlusion on several nets in Tasmania of up to about 50 % and 80 % within about one and two weeks, respectively.

The occlusion of net apertures results in additional water blockage, and several studies highlight the impact of biofouling for net drag on different scales. For example, [10] and [11] investigated the drag of clean and fouled nets in a flow and found that the drag coefficient of clean nets can increase about tenfold on heavily fouled nets. [12] measured fouling related

increase of the drag of scallop cages of up to 300 %, and [1] found fouling to cause a drag coefficient increase between 6% and 240% for a solidity escalation between 38% and 68% (corresponding to the occlusion of about 57 % to almost 80 % of net apertures). While these studies are not directly comparable due to partly unknown properties of clean and fouled nets and differences in fouling communities, they emphasize that biofouling can strongly increase loads on aquaculture nets. Consequently, biofouling also affects the loads on moorings, it can cause net deformation and it can dramatically change the hydrodynamics around and inside fish cages (e.g. [13, 14], reviewed in [2, 4, 15]). Potential effects of the accumulation of biofouling should therefore be considered when evaluating water exchange across aquaculture nets and when calculating hydrodynamic forces on cages and moorings. However, diverse and complex fouling communities complicate such an evaluation, and while methods exist to quantify overall fouling type and amount, and net aperture occlusion, information on hydrodynamic effects of specific fouling types on nets is scarce.

In order to develop better models describing the hydrodynamic effects of net fouling and to build a better basis for the implementation of net fouling into regulations and protocols for marine fish farms like the Norwegian Standard NS9415 [16] or NYTEK-forskriften [17], hydrodynamic effects of important growth types should be investigated ([1, 4]). Fouling communities on aquaculture sites are often dominated by mussels, hydroids, ascidians and algae (e.g. [3, 7, 18]). These organisms differ in size, form and flexibility and will affect the flow past nets differently. [4] investigated the effects of hydroid fouling on aquaculture nets, and the authors suggested a method to parameterize fouling to allow the use of existing clean net models to describe effects of fouling on nets.

This study aims to 1) quantify the effects of different degrees of mussel and seaweed fouling on aquaculture nets on net drag and to 2) parameterize these effects so that existing numerical models can be used to evaluate the effects of mussel and seaweed fouling. Drag was measured on a number of clean nets with different solidities and on nets fouled with varying degrees of mussel and seaweed. A comparison was then made between drag on fouled and clean nets. This allows the parameterization of fouling to describe fouling effects on drag with existing models describing the relationship of solidity, flow velocity and drag.

MATERIALS AND METHODS
Setup and procedure
Drag forces were measured on clean and fouled nets in a low-turbulence flume tank at The River and Harbor Laboratory (VHL) in Trondheim, Norway. The test parameters are summarized in Table 1.

The flume tank is 13 m long, 0.6 m wide and 0.5 m deep (Figure 1) and the water in the tank was freshwater. All nets were stretched over the sides of a rectangular aluminum frame and clamped on all sides with metal profiles as shown in Figure 2. This procedure assured minimal movement and deformation of nets during tests. The frame (0.5 m width and 0.4 m height) was made from thin, oval aluminum profiles to minimize frame drag, and it was centered in the x- and z-direction leaving a distance of 0.05 m to the tank walls at all sides.

TABLE 1: Overview over tests. All tests were conducted with a flow speed of 0.1 ms^{-1}. The drag was measured of 16 clean nets and of 24 nets with kelp fouling and 9 nets with mussel fouling. All fouled nets were of type N3 or N4 (see Table 2 in Annex).

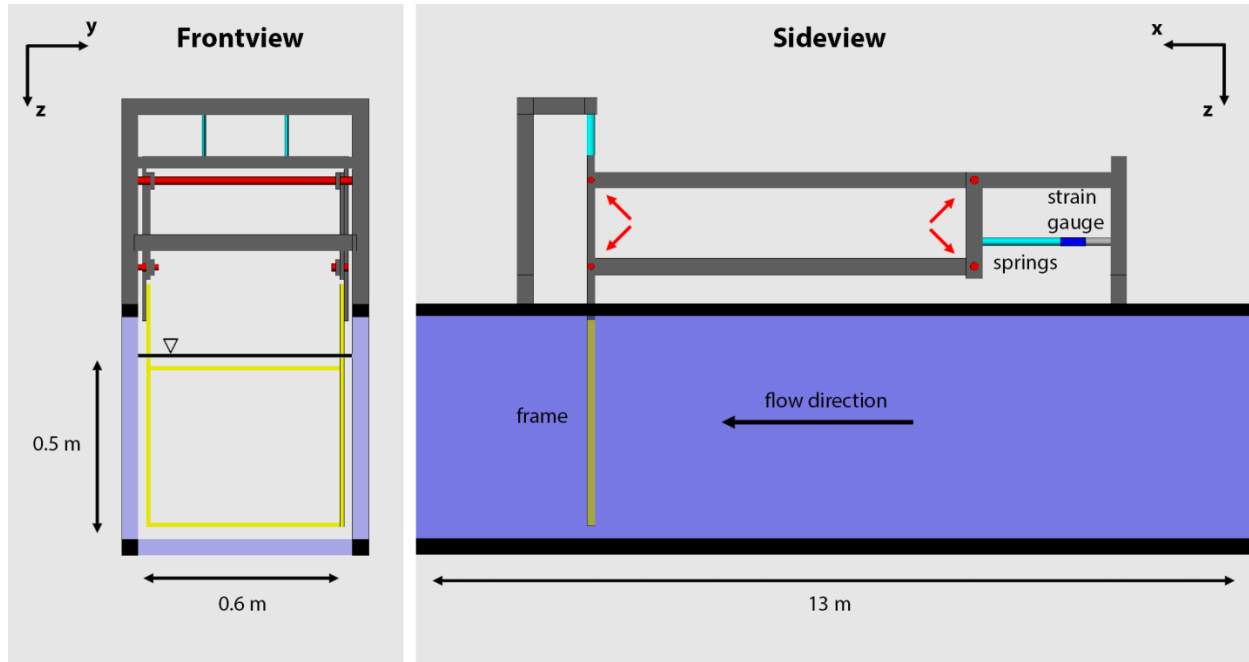| Type of net	Number of nets	Solidity range [Sn]	Current speed [m/s]
Clean, single nets	16	0.2 – 0.54	0.1
Kelp-fouled nets: lamina upstream	24	0.27 – 0.81	0.1
Kelp-fouled nets: lamina downstream	24	x	0.1
Mussel-fouled nets	9	0.31 – 0.77	0.1

Figure 1. Sketch of the flume tank with measurement setup. The strain gauges were connected to the frame via a pivoting metal parallelogram with a system of pre-loaded springs. Arrows indicate the pivot points. The distance between the tank walls and the water surface and the frame was 0.05 m on all sides.

Figure 2. All nets were mounted in a frame made from oval aluminum profiles to minimize frame drag. Fitting curved aluminum profiles were used to clamp nets to the frame. Figure 1 shows the placement of the frame in the measurement setup.

Clean and fouled nets
A) Clean nets

16 different clean nets were used and Table 2 (Annex) summarizes the solidities of all clean nets. Net solidity (S_n) is the ratio of the net area to the combined area of net strands:

$$S_n = \frac{net\ area}{combined\ strand\ area}$$

(1)

[19] derived a deterministic formulation for the calculation of the drag coefficient (C_D) of clean nets:

$$C_D = 0.04 + (-0.04 + 0.33 * Sn + 6.54 * Sn^2 - 4.88 * Sn^3)$$

(2)

In this formulation, C_D depends solely on Sn. C_D was calculated for all clean nets used in the present study from the measured forces as:

$$C_D = 2 * \frac{F_D}{\rho * v^2 * A}$$

(3)

where F_D is drag force, ρ is the density of water in the flume tank, v is the flow speed and A is the area of the net panel.

Drag coefficients for both clean and fouled nets were calculated based on eq. (3) from the drag forces measured in the flume tank. The drag coefficients found in the experiments were compared to the drag coefficients calculated from eq. (2) using

the solidity of the nets calculated using image analysis (see section *Image capture and analysis*).

B) Fouled nets

Sugar kelp (*Saccharina latissima*) was collected from Storsteinan in Mid-Norway by scuba divers and transferred to 160 L rearing tanks with aerated seawater (10 °C). To vary net solidity systematically between fouled nets, three sizes of kelp were attached to two different types of netting at four different densities. 3, 8, 15 and 25 kelp plants were attached evenly on 12 net panels of types, N3 and N4. Details about the distribution of kelp and data on clean nets are given in Tables 3 and 4 in the Annex. Kelp sizes were measured as the length of the lamina: small (12 ± 3 cm), medium (20 ± 2 cm) and large (30 ± 2 cm). The small and medium sized kelps were attached to the panel nets by fast drying glue, while the large sized kelps were attached to the nets with cable ties. The haptera (holdfast organ of the kelps) were cut to size, both to make them easier to attach to the nets, and to imitate the haptera on kelp plants growing on nets. The kelp-fouled nets were kept in the rearing tanks for few days until the drag tests were carried out and were weighed prior to the tests. Figure 3a and b show an examples of a net with kelp attached.

Blue mussels (*Mytilus edulis*) of sizes between 0.5 cm and 4.0 cm shell length were supplied by the commercial producer Norgeskjell (Åfjord, Mid-Norway). The mussels were kept in 160 L rearing tanks with 10° C aerated seawater and 24 net panels of two net types (12 panels per net type N3 and N4, see Table 3 in the Annex for details), were added allowing the mussels to attach to the surface of the nets. Different fouled net solidities were realized through non-uniform attachment of mussels between nets. An example of a net with mussel fouling is shown in Figure 3d.

Test procedure

The wet weight of all fouled nets and clean nets of type N3 and N4 was measured and the wet weight of fouling organisms on net types N3 and N4 was calculated as the difference between the weight of fouled nets and the clean net wet weight of corresponding net types.

The nets then were placed in the flume tank and images of the nets were taken under water in a current of 0.1 m/s to determine their solidity as described in section *Image capture and analysis.*

For kelp-fouled nets, underwater images of all nets in this study were taken in the current with lamina blocking net apertures on the upstream side of nets (Figure 3b), but not with lamina on the downstream side, as fouling extending downstream from nets would not be properly captured in the image analysis (Figure 3a).

Images were analyzed as described in the section *Image analysis*. The current speed was defined by setting the electrical current to the pumps in the flume tank and the speed was

calibrated to 0.1 m/s in the center of the tank using a Vectrino velocimeter (NORTEK AS, Rud, Norway; accuracy ± 0.5 % of measured value ± 1 mms^{-2}), and the flow speed was confirmed repeatedly. The nets were left in the flow for at least 5 minutes prior to measurements to minimize effects on the water flow during the installment of nets. The (in-line) drag of nets and frame was measured with two strain gauges (AEP transducers, Cognento, Italy; model TCA.315.R3, Code: CTCA5K5; repeatability ≤ ± 0.01 %; linearity and hysteresis ≤ ± 0.03 %) for 120 seconds per test at a sampling frequency of 100 Hz. The strain gauge signals were amplified and transferred to a PC via a HP3852 data acquisition system using HP44726A multiplexers (Hewlett Packard Inc., Palo Alto, USA). The drag on all clean and mussel-fouled nets was measured once, while the drag on all kelp-fouled nets was measured once with lamina downstream from (see Figure 3a) and once with lamina upstream of (see Figure 3b) the net. The drag on the empty frame was measured to allow the calculation of the drag on the nets only as described in section *Data processing*.
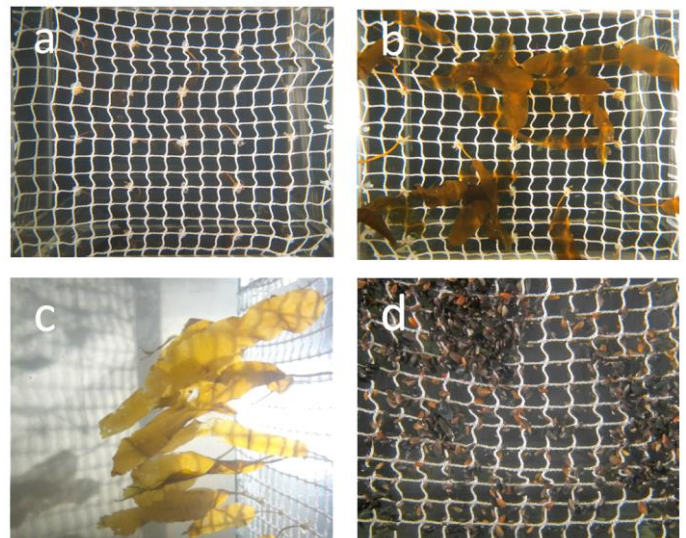

Figure 3. Behavior of kelp in a current from the opposite side of kelp attachment (a, c) and from the side of kelp attachment (b). The images are taken in direction of the current. The kelp plants align with the current when water flows through the net from the side opposite to the attachment of the stipes, while the lamina are pressed against the net when the current direction is from the side of kelp attachment. An example of mussel fouling on a net is shown in panel d.

Image capture and analysis

The lighting of a scene defines how bright objects in an image appear. Dynamic range is defined by the difference in brightness levels of a scene an imaging sensor is able to capture. If the variation of brightness levels in a scene exceeds the dynamic range of the imaging sensor, data will be lost leaving some objects completely black and/or others completely white. The image analysis method used in the present study aims to

find the relationship of pixels belonging to nets and fouling to pixels belonging to the background (net apertures). The setup was similar to that described in [4]. A strong set-light was used to evenly illuminate nets, minimizing variations in brightness levels on nets and fouling throughout the image, to achieve good contrast to the background. Other factors affecting the results are image blur (sharpness) and Depth of Field (DOF), image resolution, ISO settings, in-camera image processing (hue/saturation adjustment, sharpening, data compression, noise cancelling etc.), and sensor parameters such as intrinsic noise, pixel density and physical dimensions. Sharpness and DOF are the most important of these factors, as edge detection is used to determine the border of objects, which is based on a threshold for this difference in contrast. The correct threshold must be carefully decided, since the wrong threshold will affect the classification of pixels as foreground or background pixels, thereby degrading the accuracy of the results. To optimize the image quality with respect to image analysis for solidity calculations, a small aperture (large DOF and more forgiving when automatic focusing is not accurately on the net plane) was chosen along with standardizing the camera position perpendicularly to the net in the flume tank. All images were taken with a Canon Powershot G12 digital camera (Canon Inc., Tokyo, Japan), with a resolution of 3648 x 2736 pixels in RAW format.

The image analysis followed the description by [20], with some minor changes. Images were taken of all nets stretched onto the measurement frame and mounted in the flume tank and with a flow speed of 0.1 ms^{-1}. RGB (Red, Green, Blue) images were converted to HSL (Hue, Saturation, Luminance) color space and the luminance channel was used for segmentation using manual thresholding. Segmented binary images contained white (net and fouling) and black (background) pixels and solidity were calculated from the ratio of white to black pixels to the total pixel count of the images. Solidity was expressed as:

$$Sn = \frac{white\ pixels\ (area\ of\ net\ strands\ and\ fouling)}{total\ pixel\ count\ (total\ area\ within\ the\ net\ outline)} \quad (4)$$

See [20] for a more detailed description of the method.

Data processing and correlations

The time averaged total force on the frame and nets was calculated as the sum of the mean values of the filtered time series' from both strain gauges. The forces on the bare frame were subtracted from the forces obtained from tests with net samples.

The solidity contribution of kelp on fouled nets was compared with the corresponding wet weight of net panels to find a correlation between the two measures. Assuming wet weight to be associated with seaweed surface area, increasing wet weight may lead to higher rates of overlapping seaweed. Increasing overlap would lead to an increasingly non-linear relationship between wet weight and solidity, and solidity would increase at slower rates when wet weight increases. Nonetheless, the coefficient of determination (R^2) of a linear regression analysis was calculated to describe the spread of data around the best linear fit. Linear regression was chosen because a near-linear relationship between wet weight and solidity occurs when the same increase in weight of fouling leads to approximately the same increase in solidity. This assumption is valid as long as i) the 2-dimensional area to weight ratio of fouling organisms is constant for a given fouling organism of a given size and ii) an increase of fouling organisms does not lead to increased levels of overlap of fouling organisms in the images, assuming that the percentage of overlap of organisms is constant. The relationship between wet weight and solidity did not indicate a clear effect of overlap under certain cutoff wet weights from which on solidity stayed relatively stable (Figure 5).

RESULTS
Clean nets

The drag coefficient, based on the overall net area, of all clean nets is shown in Figure 4. The drag coefficient increased with increasing net solidity, and C_D of all nets is close to the drag formulation by [19], Eq. (2). It should be noted that Eq. (2) was developed based on a number of tests with knotted nets in the solidity range from $Sn = 0.13$ to $Sn = 0.32$, while the present study uses Raschel type nets (without knots) with solidities up to $Sn = 0.54$.
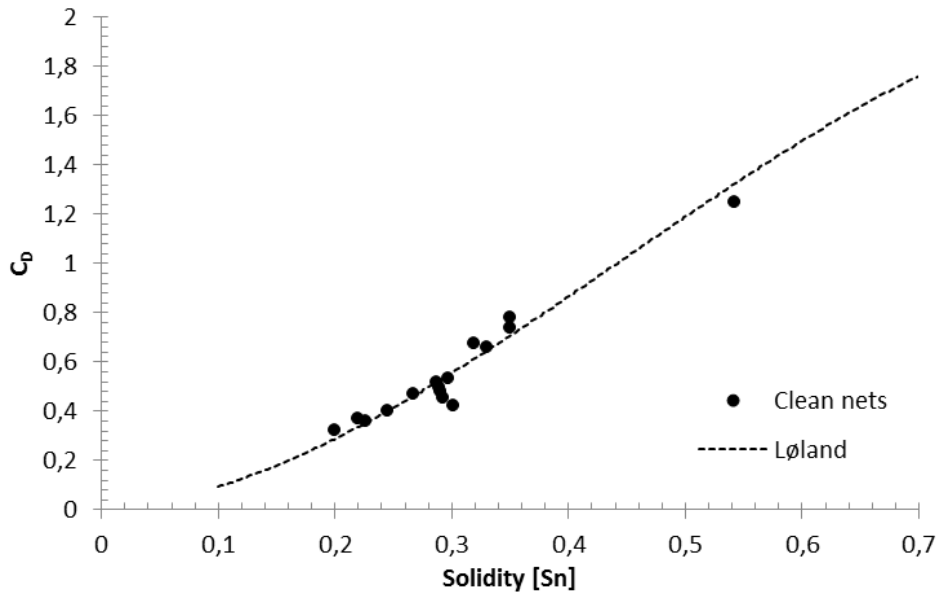
Figure 4. Drag coefficients of clean nets and expected drag based on the formulation by [19]; dashed line, Eq. (2)). Net characteristics are summarized in Table 2 (Annex).

Kelp

The solidity contribution of kelp, that is the part of the net solidity that is caused by fouling, increases with kelp wet weight for both fouled net types, N3 and N4 (Figure 5). This relationship changes around 1300 gm^{-2}. From this wet weight on solidity contribution does not further increase with wet weight, but it is within a range between $Sn = 0.37$ and $Sn = 0.52$. The maximum solidity contribution differed between the net types, with a higher maximum solidity contribution on net type N4,

which has a higher solidity. The grey and hatched areas in Figure 5 depict ranges in which the data, despite a relative small number of data points, indicates that increase in wet weight does not increase solidity of the net panel. Up to about 1300 gm^{-2}, linear models describe the relationship between solidity contribution of kelp and wet weight reasonably well for both nets, but there is considerable spread of data around linear fits (linear regression; N3: $R^2=0.80$, N4: $R^2=0.73$).
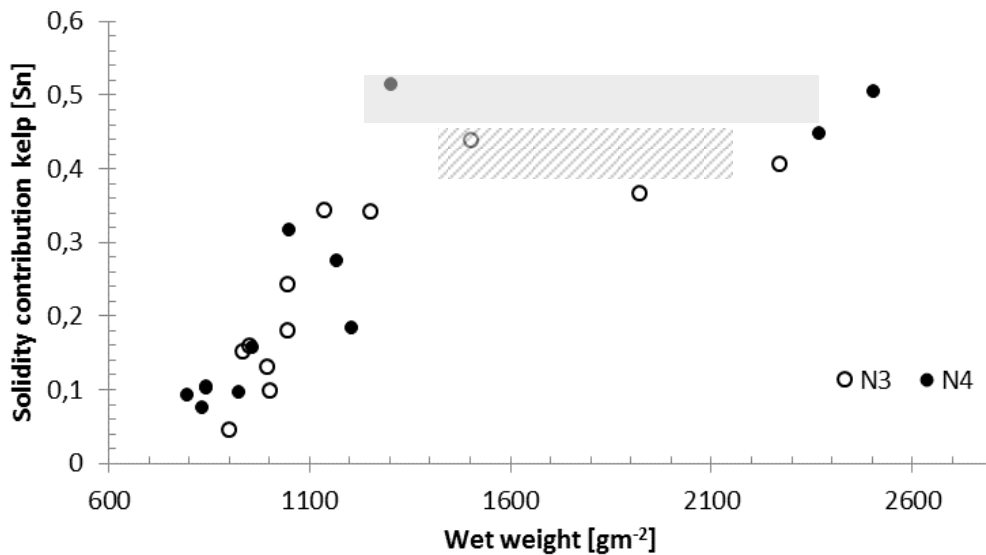

Figure 5. Relationship of wet weight and solidity contribution (Sn of fouled net – Sn of original, clean net) for kelp-fouled nets. Two net types were fouled: N3 and N4 (see Table 2, Annex).

Figure 6 shows the relationship between solidity and drag on kelp-fouled nets with the current pressing lamina against the net (a) and with lamina standing in the current downstream from the nets (b). When kelp are pressed against the net by the current, the relationship between net solidity and drag is very close to expected results for clean nets based on Eq. 2 ([19]) (Figure 6a) for both net types. However, within the tested solidity range also simpler linear fits describe the relationship between solidity and drag well, and there is relatively little scatter around linear fits (linear regression; N3: $R^2 = 0.95$, $p < 0.01$ N4: $R^2 = 0.92$, $p < 0.01$). When the current was in the opposite direction, and the lamina were downstream from the nets, drag was lower (Figure 6b) and there was some more scatter around linear fits

(linear regression; N3: $R^2 = 0.41$, $p < 0.05$, N4: $R^2 = 0.81$, $p < 0.01$). It should be noted that the solidity in Figure 6b is the solidity of net panels with kelp being pressed against the net (same solidity measure as for Figure 6a), and that solidity is simply used as a rough measure for the amount of fouling to allow a simple comparison of the drag on nets with the current from opposite directions. Figure 6 shows the relationship between solidity and drag based on Eq. (2) for comparison. The difference between expected clean net drag based on Løland's formulation ([19], Eq. (2)) and the measured drag on kelp-fouled net panels with kelp extending downstream from the nets (Figure 6b) increased with increasing solidity.
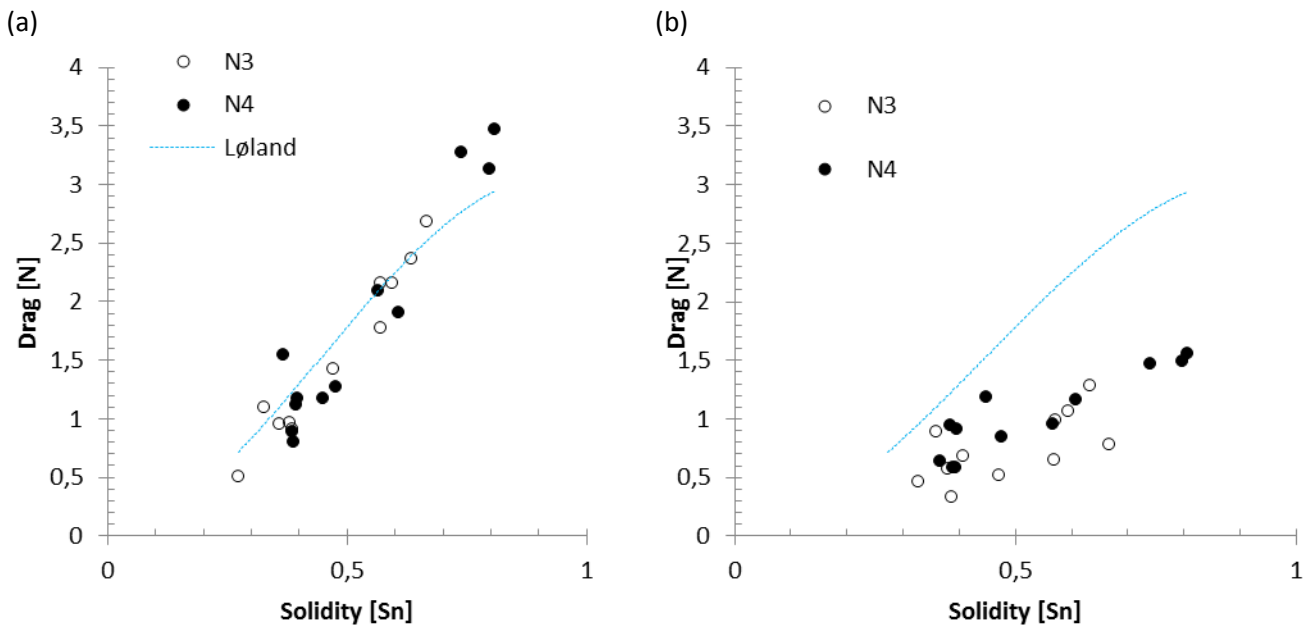

Figure 6. Drag on kelp-fouled nets (types N3 and N4, see Table 2, Annex) in dependence of fouled-net solidity. Solidity was measured with the flow from the net side where kelp was attached, that is with kelp pressed against the net. Drag on the nets was measured upstream and downstream of the flow direction. That means kelp was pressed against the nets in (a) and was stretched out into the current direction downstream from the nets in (b). The dashed lines are theoretical results for clean nets based on a formulation by Løland (Eq. (2)).
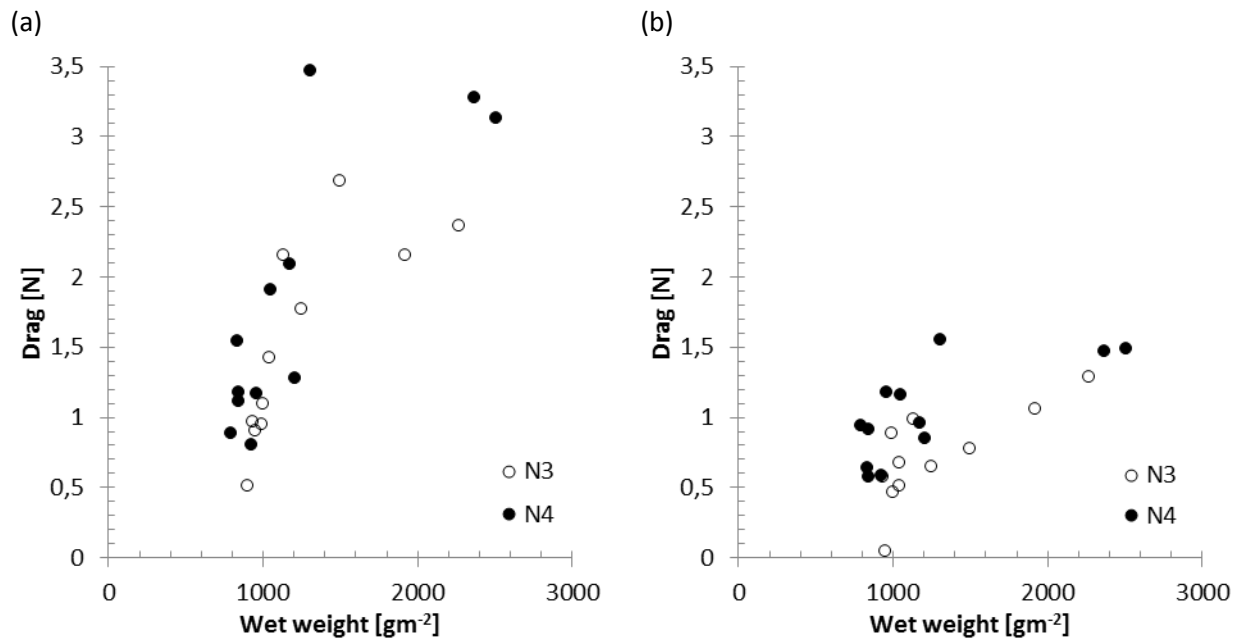
Figure 7. Drag on kelp-fouled nets (types N3 and N4, see Table 2, Annex) in dependence of fouling wet weight. Drag on the nets was measured with the flow in two different directions, as described for Figure 6. That means kelp was pressed against the nets in (a) and was stretched out into the current direction downstream from the nets in (b).

Drag varied strongly within a narrow range of wet weight of $800 - 1300$ gm^{-2} (Figures 7a and b) and there seemed to be a tendency for little change in drag with increasing wet weight at highly fouled nets with wet weights exceeding 1300 gm^{-2}. Regression analysis on the relationship between wet weight and drag therefore only takes into account nets with wet weights up to 1300 gm^{-2}. When kelp lamina where pressed against the net by a current, drag generally increased with increasing wet weight (Figure 7a), but there was a substantial amount of scatter around linear fits, especially for net type N4 (linear regression;

Blue mussels

Mussels were attached to nets in clusters on both sides of the nets. On a number of net panels considerable amounts of mussels were lost during tests and all of these nets were removed from the study. As a result, the amount of available data was restricted, and most of the data is for wet weights < 2500 gm^{-2} (Figure 8 and Table 4 in the Annex). Solidity of mussel-fouled nets was between $Sn = 0.31$ and $Sn = 0.77$, and solidity was more evenly distributed than wet weight (Figure 9 and Table 4 in the Annex).

N3: $R^2=0.87$, $p < 0.01$, N4: $R^2=0.58$, $p < 0.05$). When kelp lamina where on the downstream side of nets, there was no significant linear relationship between wet weight and drag for nets with wet weight below 1300 gm^{-2} (linear regression; N3: $R^2=0.17$, $p = 0.31$, N4: $R^2=0.39$, $p = 0.053$). However, in this flow situation, net type N3 did not show a clear tendency for little change of drag at high wet weights (Figure 7b). When all nets N3 are taken into account, regression analysis reveals a positive linear relationship between wet weight and drag with substantial scatter around a linear fit ($R^2=0.58$, $p < 0.01$).

The relationship between wet weight and solidity contribution by blue mussels on the nets is shown in Figure 8. Solidity contribution of mussels to the overall net solidity increased with increasing mussel wet weight. More data would be necessary to safely identify a ratio or function describing the relationship of weight and solidity, especially since large differences of this relationship between net types N3 and N4 suggests an effect of net type.
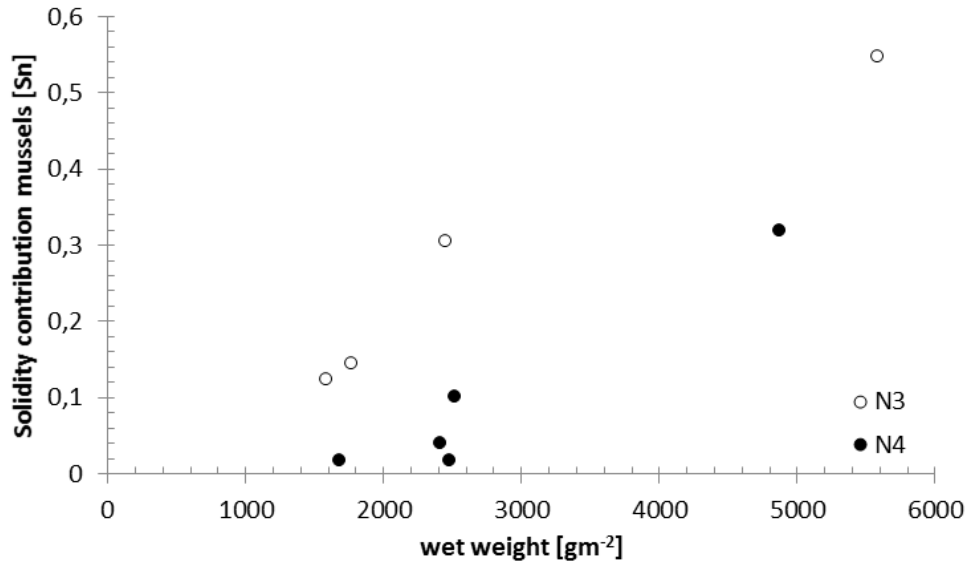
Figure 8. Relationship of wet weight and solidity contribution (Sn of fouled net – Sn of original, clean net) for mussel-fouled nets. Two net types were fouled (N3 and N4, see Table 2, Annex).

Drag on mussel-fouled nets increased with solidity (Figure 9a). Low amount of data per net type restricts any proper statistical analysis, but drag generally increased with solidity for both fouled net types. Furthermore, the drag on all mussel-fouled nets was close to drag of clean nets with similar solidities based on Løland's drag formulation ([19], Eq. (2)), even though the solidity of most fouled nets was outside of the solidity range in which Eq. (2) strictly is validated in. The maximum difference to clean net results based on Løland [19] was under 30 % and

2/3 of all data were within 15 % of the clean net result calculated using Eq. (2).

Data for net types N3 and N4 overlaps, and net type does not seem to have a major effect on the relationship between solidity and drag. However, due to few data points no statistical analysis was performed to confirm this.
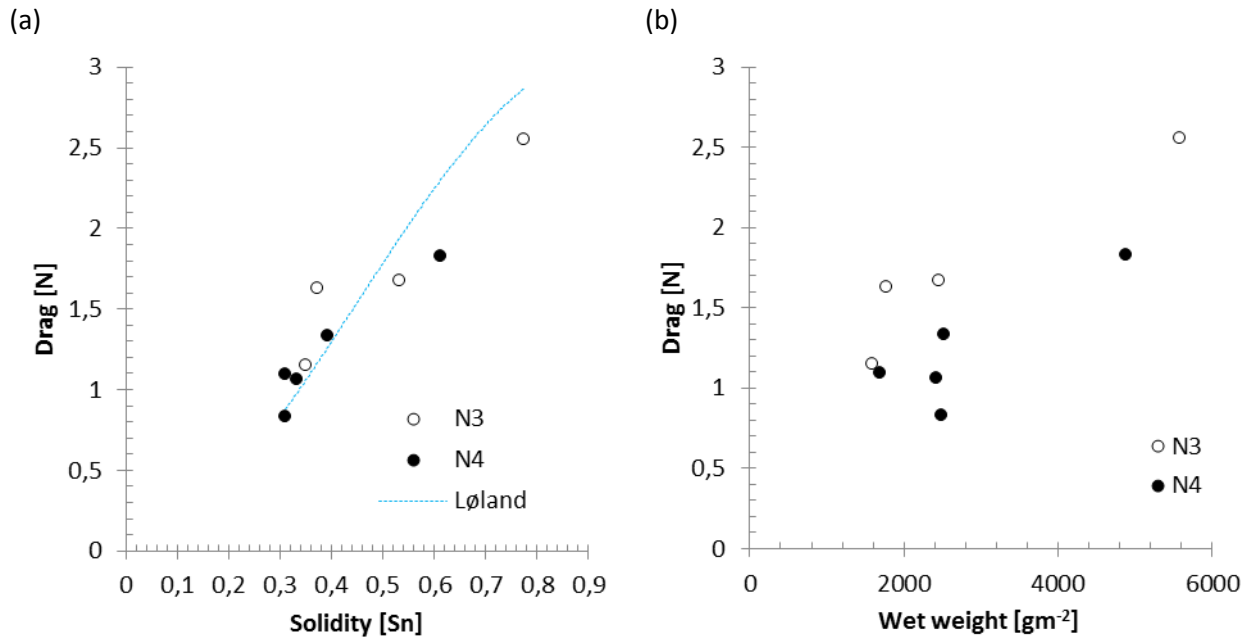

Figure 9. Drag on mussel-fouled nets in dependence of solidity (a) and wet weight (b) for two net types (N3 and N4, see Table 2, Annex). The dashed line shows theoretical results for clean nets based on a formulation by Løland (Eq. (2)).

DISCUSSION
Tank setup
Flume tanks have some limitations that are important to be aware of. Propellers or impellers are used to circulate the water. This and the redirection of the water when it passes from outlet to inlet can induce turbulence and a non-uniform flow field. In addition there will be a shear layer on the walls and bottom of the tank. In our tests the latter effect may influence our results due to the relatively small distance between the net and frame and the walls and bottom of the tank. The relatively small distance between the test object and the walls and bottom may also create blockage effects. A porous body such as the net will to some degree change the direction and velocity of the flow in the vicinity of the net, meaning that in a free flow some of the water may be directed around the net itself. This effect is dependent on the solidity of the net and the flow velocity. If the walls of the tank are close enough to the net the flow velocity through the net and between the frame and tank walls and bottom may be higher than in a free flow, thus affecting the drag forces on the net. This effect will increase with increasing solidity (including the effect of biofouling). In addition to close proximity to the walls and bottom of the tank, being close to the free surface may generate surface waves and thus added resistance on the net.

Evaluating the effects on drag from the above mentioned factors are difficult. Even with extensive measurements of flow velocities in the tank, estimating the effects would not be trivial. One would normally make sure that the distance to tank walls, bottom and free surface are large enough for these effects to be negligible. This was not possible in our work due to availability of tanks where we could use biological material and the size of net panel needed for attaching fouling and testing the effects on the drag forces. The details of these effects were not investigated further, but we will evaluate the effects qualitatively. Due to the low flow velocity and that no waves were observed visually the effect of being close to the free surface are thought to be small. The effect of a shear layer are also thought to at most only affect a small portion of the net. The largest effect on drag forces will most likely be blockage effects due to proximity to the tank walls and bottom. Although the effect may be small for lower solidities, the effect may increase with increased solidity of the net (including fouling). Although this introduce an uncertainty in our results it is thought that we still can assess the qualitative differences between clean nets and different types of and degree of fouling. The results in this study may then be conservative for higher solidities, meaning higher drag forces compared with tests where the effects of tank walls and bottom are negligible. This being said, there may be benefits in running tests where transverse flow around the net is restricted due to close proximity to walls and bottom. This test setup may qualitatively be better able to represent the net panel as a small part of a larger net, although the blockage effect introduce an error source that one might need to account for. Further investigation of the effect on drag forces due to test setup is needed to clarify restrictions and benefits for each method. Future experiments with biodouling should also include the effect of Reynolds number on the drag forces. Such tests should include a variety of flow speeds..

Clean nets
Several authors investigated the drag on clean nets. A number of different deterministic formulations for the calculation of C_D were derived based on net solidity and current velocity (e.g. [19, 21, 22]). This study compares the drag coefficient measured on 16 different clean, knotless nylon nets with drag coefficients for nets with similar solidities based on a formulation by Løland [19]. Løland's formulation was chosen, as it was derived from tests over a wide range of solidities (Sn=0.13 to Sn=0.32) and included tests at a relevant flow speed (0.159 ms^{-1}) and, with net twine diameters in the range of millimeters, at relevant Reynolds numbers. Twine diameters of nets in the present study were within the range between 1.08 mm and 3.00 mm, giving a Reynolds number range between roughly 100 and 260, while assuming the twine shape to be cylindrical. Within this Reynolds number range the drag coefficient of long cylinders changes with only a few percent ([23]). This indicates that it is appropriate to compare the drag on nets used in this study, but differences in twine diameter may contribute to some scatter. Even though Eq. (2) (Løland's formulation) is, strictly speaking, valid only for solidities up the Sn=0.32 [19], it describes the relationship between net solidity and flow speed well for all nets in the present study up to Sn=0.54 (Figure 4). This indicates that i) Løland's formulation ([19]) may be applicable to nets with high solidities and that ii) the measurement setup was functioning and well calibrated. It should be mentioned that [4] found Løland's formulation ([19], Eq. (2)) to underestimate the drag on a net with Sn > 0.4. This difference to the present data indicates that solidity may not be the only factor influencing drag on highly solid nets, but also differences in test setups may play a role. Some slight deviations of single measurements from the expected drag may be due to differences in the flow structure around the twines of different nets, as suggested by [4]. However, there was only slight scatter and this was not further investigated in this study.

Fouled nets
Kelp
Kelp biomass increase is mostly associated with an increase of the total lamina area [24]. When a large percentage of net apertures is already occluded by kelp, additional lamina area is likely to overlap with these areas, rather than to cover only open net area. This fits with the finding of the present study that the relationship between kelp wet weight and net solidity approaches a maximum solidity, from which on net solidity is largely independent from wet weight (Figure 5). Therefore, the relationship between wet weight and the net area covered by kelp is not only dependent on wet weight, but also on the amount of fouling. The nets used in this study are within the

solidity range commonly used in salmon farming. For such nets the relationship between wet weight and solidity seems to be roughly linear up to a solidity contribution of kelp of about $0.4 - 0.5$ or a wet weight of about 1300 gm^{-2}. This critical weight may not be absolute for any net with kelp fouling, but it may dependent on the state, size and distribution of kelp.

The drag of kelp-fouled nets with lamina pressed against the nets was close to the relationship between solidity and drag for clean nets as described by [19], and data from both net types overlapped (Fig. 6a). That means that the relationship between solidity and drag for kelp-fouled nets is described well with the clean net model by [19] as long as all kelp lamina are perpendicular to the flow on the upstream side of the net. Therefore, original clean net solidity has no or little influence on the relationship between solidity and drag on the fouled nets when all lamina are pressed against the net perpendicular to the flow. That implies that drag increase due to kelp lamina blocking the flow through an area of the net panel is close to that of net twines blocking a similar area, as otherwise differences in the initial clean net solidity would cause an offset in the drag between different nets.

Lamina closing net openings cause total water blockage in these areas and a flow around the lamina, leading to pressure differences on the upstream and downstream side that are associated with net drag, similarly to the effect of an impermeable plate. Lamina extending downstream from a net in a current do not block water in the same way, but skin friction along the lamina surface leads to drag on the kelp. Therefore, the drag on nets in this situation is much lower (Fig. 6 a and b). Also, the correlation between solidity (measured as overall net solidity with lamina pressed against the nets) and drag is worse when lamina extend downstream from nets, as indicates by a lower coefficient of determination (R^2 was 0.95 and 0.92 for net types N3 and N4 with lamina pressed against the net and 0.41 and 0.81 for these nets with lamina on the downstream side).

Even though seaweed lamina extending downstream in a current may move in the flow, the standard deviation of the drag time series in terms of percent of the average drag is similar for both flow directions (2.2 % on average for lamina downstream in the flow, 2.3 % on average for lamina pressed against the net; Table 3 in annex). That means that flow direction does not strongly affect overall variability around the average drag on a seaweed-fouled net. Furthermore, standard deviation was similar to that of clean net drag time series, which means that the relative size of fluctuations of drag over time is similar for clean nets and seaweed-fouled nets.

However, the average drag increase with solidity is more variable when lamina are attached on the downstream side of a net. Then, factors other than only solidity influence drag and therefore solidity alone is less reliable as a measure to estimate net drag. In contrast, solidity seems to be a good measure for the estimation of net drag when lamina are pressed against the net.

Linear correlation of wet weight and drag ($R^2 = 0.58$ and $R^2 = 0.81$ for net types N3 and N4) was lower than that of solidity and drag ($R^2 = 0.95$ and $R^2 = 0.92$ for net types N3 and N4) when kelp lamina were pressed against the net on the upstream side. When kelp was attached on the downstream side of nets, there was no linear relationship between wet weight and drag when considering all nets with wet weights lower than 1300 gm^{-2}.

That means that wet weight, even though weight is associated with lamina area, is not a suitable measure for the estimation of drag on kelp-fouled nets when lamina are attached on the downstream side of nets. When all kelp are attached on the upstream side and lamina are closing net apertures, wet weight may allow a very rough estimation of net drag. However, the coefficient of determination for linear regression analyses for nets of type N3 and N4 differed substantially and were relatively low and wet weight as a measure for the estimation of net drag should be used cautiously even when all fouling is attached to the upstream side of nets. Since wet weight alone does not give any information about the distribution of kelp and about kelp-related blockage of net apertures, a high amount of scatter in the relationship between wet weight and drag is expected. Solidity, on the other hand, is a measure for net blockage and a much better measure for the estimation of net drag.

In the field, kelp may attach to both sides of the net and in a current some lamina may cover net openings on the upstream side, while some lamina may extend away from the net on the downstream side. Net solidity based on underwater images may not detect lamina that stand far back in a current, which will contribute to the overall net drag. Thus, the drag estimated from the relationship shown in fig. 6a can be underestimated for field tests. However, kelp on the upstream side of nets will have a much stronger effect on net drag than kelp on the downstream side. A rough estimation of kelp effects on drag shows that lamina attached to the upstream side of nets may contribute two to three times more to the net drag than lamina on the downstream side, assuming that fouling is evenly distributed on both sides and it leads to a doubling of the initial net solidity of $Sn = 0.3$ in a flow of 0.1 ms^{-1} (see Annex for more detailed estimation).

Blue mussel
Only few data points were available to compare the relationships between wet weight, solidity and drag of nets fouled with blue mussels, as a large number of nets had to be removed from this study. Nonetheless, some conclusions can be drawn from the present tests regarding the effects of mussel fouling on net drag. The average standard deviation within time series was about 1.8 % of the average drag for mussel fouled nets, which is even lower than the average standard deviation for clean nets (2.4 %; Tables 2-4 in annex), which suggests that mussel fouling generally does not contribute to temporal fluctuations of the hydrodynamic force acting on fouled nets in a steady current.

Figure 8 shows that there was high variability of the relationship between wet weight and net solidity even for a given net type; three nets of type N3 had almost the same wet weight of mussels, but the solidity contribution of the mussels was between 0.02 and 0.1. Furthermore, the same wet weight of blue mussel can give different solidity contributions on different nets (see Figure 8). Assuming only minor differences between characteristics of mussels on the nets (like different average density) this means that clean net characteristics seem to affect the relationship between mussel wet weight and net solidity, at least when mussels contribute little to the overall net solidity. These findings are also reflected in the relationship between wet weight and drag (Figure 9b), which shows adifference in the effect of wet weight on drag between the two net types, but to a lesser extend. For a given amount of fouling there was higher drag on the less solid net type (N3). However, with substantial scatter (especially for net N4) and few data points any conclusion on effects of the net type should be drawn carefully. . Due to the scatter in the relationships between wet weight and solidity contribution and wet weight and drag, wet weight does not seem to be a good measure for the estimation of drag on mussel-fouled nets in a current.

In contrast, there is no clear difference between the net types in the relationship between solidity and drag (Figure 9a). For solidities up to about 0.4 this relationship is described well by the clean net drag formulation by [19], while this formulation seems to overestimate the drag on nets highly fouled by blue mussels. This is slightly different from the seaweed results, where the drag on fouled nets at low solidities was slightly lower (Figure 6a), but at high solidities the drag formulation by [19] underestimates measured drag on nets fouled with seaweed. We did not properly investigate the flow past mussels and seaweed and can therefore not discuss possible reasons for these differences in detail, but they may arise from a very different geometry of seaweed blades and mussel fouling. These differences might lead to different wake properties (wake widths) and therefore differences in the flow speed reduction behind seaweed and mussels. There is little data for mussel-fouled nets at high solidities and findings based on the present data alone should not be overrated. However, there is relatively little scatter in the relationship between solidity and drag for mussel-fouled nets, even when all data from both net types is evaluated together. One important reason for little scatter is in the nature of the relationship between solidity of mussel fouled nets and drag: mussel fouling is hard fouling and solidity is associated directly with water blockage, which is assumed to be the main factor to influence drag. Furthermore, mussel fouling in the 2-dimensional plane normal to the camera view can be captured entirely in a single image, as long as proper illumination allows for an aperture setting resulting in a suitable DOF, and there is little change with time in the structure of the net and mussels in a constant flow. This will reduce the error that is introduced to solidity measurements by the fact that a picture only allows the evaluation of a brief moment in time, as this error will depend largely on the variability of the positioning of fouling organisms over the measurement period. Based on the limited data collected in this study, solidity seems to be a good measure for the estimation of drag on mussel-fouled nets.

Application
[4] describe the effect of hydroid-fouling on net drag and they suggest a method to parameterize fouling using drag as a proxy. Based on their discussion the current data may be used in much the same way.
Models exist describing the relationship between clean net characteristics and drag. Such models are used for the calculation of hydrodynamic forces on net structures and for the estimation of the behavior of net cages in the sea. The formulation by [19] describing the relationship between solidity and drag for clean nets also describes the relationship between these parameters reasonably well for nets fouled with kelp (when all lamina are pressed against the net) and blue mussels, and therefore this formulation may be used directly to roughly estimate the effect of kelp- and mussel-fouling on nets. Using Løland ([19], Eq. (2)) or another functions describing similar relationships, a given fouled net can be matched with a clean net that experiences similar drag under similar conditions. The solidity of this clean net is the *effective clean net solidity* of the fouled net. The drag on a fouled net can then be estimated by calculating the drag on a clean net with the effective clean net solidity of the fouled net, using existing models that describe the relationship between solidity, flow velocity and drag. While the present study suggest that Eq. (2) may be used for a rough estimation of the effective solidity of mussel- and seaweed fouled nets (as long as seaweed are pressed against the net by a current perpendicular to the net), other types of fouling may influence solidity and drag differently, as for example shown for hydroids [4].
Knowledge about the effective solidity of fouled nets can provide input to risk based maintenance schemes by eliminating subjective opinions related to when a net should be cleaned. Automated solidity calculations based on image segmentation can give an objective measure of solidity which has an effect on drag force on the net and water flow through the cage. This will aid the decision making process related to mechanical load and fish welfare.
A more detailed description including a general description of how to find transfer functions between clean and fouled net data is found in [4].

CONCLUSIONS
The relationship between net solidity of and drag on clean nets tested in the present study is well described by the drag formulation by [19], even for solidities exceeding the validated range of solidities of this formulation. Solidity and wet weight are frequently used to quantify biofouling. While wet weight describes the total amount of biofouling, solidity gives information about the distribution of fouling in two dimensions. The relation of these two methods is dependent on the type of

fouling and it can depend on the type of net (as seen for mussel-fouled nets in this study). Drag on nets generally increases with wet weight of kelp and blue mussel, but correlation between these measures was low. Drag on fouled nets will largely depend on the distribution of fouling, which may be variable also for similar amounts of a certain type of fouling on similar nets. This is likely the major cause for low correlation between wet weight and drag.

Solidity as a measure for the amount of fouling on nets has limitations, as the effect a certain increase of fouling has on solidity depends not only on the amount of fouling increase, but also on the initial net solidity. Also, solidity has an absolute upper limit (when all net apertures are fully occluded), from which a further increase of fouling on a net does not lead to increased solidity. However, solidity correlates well with the drag on kelp- and mussel-fouled nets, at least as long as fouling organisms are mainly close to the net and do not extend far downstream. The blockage of water through the net has a major impact on drag. Since solidity gives information about the distribution of fouling, it is (according to the results in this study) a much better measure for the estimation of drag on nets than wet weight.

Knowledge about the effect of a given type of fouling on the drag on nets allows the use of drag as a proxy to find transfer functions between fouled and clean net solidity. That means this knowledge enables us to use models developed to describe the effect of clean net solidity on drag to model the effect of fouling. The relationship between solidity and drag for nets fouled with mussels and kelp (pressed against the net on the upstream side) was reasonably well described with linear fits, but it was also similar to the description of the relationship between solidity and drag given by Eq. (2). Therefore, Lølands formulation for clean nets ([19], Eq. (2)) may also be used to roughly estimate the effect of kelp and mussel fouling on nets.

ACKNOWLEDGMENTS

REFERENCES
[1] Swift, M. R., Fredriksson, D. W., Unrein, A., Fullerton, B., Patursson, O., and Baldwin, K., 2006, "Drag force acting on biofouled net panels," Aquacultural Engineering, 35(3), pp. 292-299.

[2] de Nys, R., and Guenther, J., 2009, "The impact and control of biofouling in marine finfish aquaculture," Advances in Marine Antifouling Coatings and Technologies, C. Hellio, and D. Yebra, eds., Woodhead Publishing, Cambridge, UK, pp. 177-221.

[3] Fitridge, I., Dempster, T., Guenther, J., and de Nys, R., 2012, "The impact and control of biofouling in marine aquaculture: a review," Biofouling, 28(7), pp. 649-669.

[4] Gansel, L. C., Plew, D. R., Endresen, P. C., Olsen, A. I., Misimi, E., Guenther, J., and Jensen, Ø., 2015, "Drag of Clean and Fouled Net Panels – Measurements and Parameterization of Fouling," PLoS ONE, 10(7), p. e0131051.

[5] Greene, J. K., and Grizzle, R. E., 2007, "Successional development of fouling communities on open ocean aquaculture fish cages in the western Gulf of Maine, USA," Aquaculture, 262(2-4), pp. 289-301.

[6] Madin, J., Chong, V. C., and Hartstein, N. D., 2010, "Effects of water flow velocity and fish culture on net biofouling in fish cages," Aquac. Res., 41(10), pp. e602-e617.

[7] Bloecher, N., Olsen, Y., and Guenther, J., 2013, "Variability of biofouling communities on fish cage nets: A 1-year field study at a Norwegian salmon farm," Aquaculture, 416–417(0), pp. 302-309.

[8] Braithwaite, R. A., Carrascosa, M. C. C., and McEvoy, L. A., 2007, "Biofouling of salmon cage netting and the efficacy of a typical copper-based antifoulant," Aquaculture, 262(2-4), pp. 219-226.

[9] Hodson, S. L., Lewis, T. E., and Burke, C. M., 1997, "Biofouling of fish-cage netting: Efficacy and problems of in situ cleaning," Aquaculture, 152(1-4), pp. 77-90.

[10] Milne, P. H., 1970, Fish farming: a guide to the design and construction of net enclosures, H.M. Stationary Off., Edinburgh, Great Brittain.

[11] Baldwin, K. C., Celikkol, B., Swift, M. R., Fredriksson, D., Tsukrov, I., and Ieee, 2003, Open ocean Aquaculture engineering II, Marine Technology Soc, Washington.

[12] Yamamoto, K., Hiraishi, T., and Kojima, T., 1988, "STUDIES ON THE OPTIMUM DESIGNS OF THE MARINE CULTURE FACILITIES .1. DRAG OF A NET CAGE ENCRUSTED WITH MARINE ORGANISMS IN SCALLOP CULTURE," Nippon Suisan Gakkaishi, 54(11), pp. 1913-1918.

[13] Fredheim, A., 2005, "Current Forces on Net Structure," PhD Doctoral thesis, NTNU, Trondheim, Norway.

[14] Lader, P., Dempster, T., Fredheim, A., and Jensen, Ø., 2008, "Current induced net deformations in full-scale sea-cages for Atlantic salmon (Salmo salar)," Aquacultural Engineering, 38(1), pp. 52-65.

[15] Klebert, P., Lader, P., Gansel, L., and Oppedal, F., 2013, "Hydrodynamic interactions on net panel and aquaculture fish cages: A review," Ocean Engineering, 58(0), pp. 260-274.

[16] 2009, "Norwegian Standard NS9415.E:2009 Marine fish farms - requirements for site survey, risk analyses, design, dimensioning, production, installation and operation.," Standard Norge, Lysaker, Norway, p. 108.

[17] Lovdata, 2011, "Forskrift om krav til teknisk standard for flytende akvakulturanlegg (NYTEK-forskriften) (Norwegian)," I. a. F. Ministry of Trade, ed., Lovdata.

[18] Braithwaite, R. A., and McEvoy, L. A., 2005, "Marine biofouling on fish farms and its remediation," Adv Mar Biol, A. J. Southward, P. A. Tyler, C. M. Young, and L. A. Fuiman, eds., Academic Press Ltd-Elsevier Science Ltd, London, pp. 215-252.

[19] Løland, G., 1991, "Current Force on and Flow through Fish Farms," Dr. Eng., The Norwegian Institute for Technology, Trondheim.

[20] Guenther, J., Misimi, E., and Sunde, L. M., 2010, "The development of biofouling, particularly the hydroid *Ectopleura larynx*, on commercial salmon cage nets in Mid-Norway," Aquaculture, 300(1-4), pp. 120-127.

[21] Aarsnes, J. V., Rudi, H., and Løland, G., 1990, "Current forces on cage, net deflection," Engineering for Offshore Fish Farming, Thomas Telford, London, pp. 137-152.

[22] Milne, P. H., 1972, Fish and Shellfish Farming in Coastal Waters, London.

[23] Schlichting, H., 1979, Boundary Layer Theory, McGraw-Hill, New York, USA.

[24] Bartsch, I., Wiencke, C., Bischof, K., Buchholz, C. M., Buck, B. H., Eggert, A., Feuerpfeil, P., Hanelt, D., Jacobsen, S., Karez, R., Karsten, U., Molis, M., Roleda, M. Y., Schubert, H., Schumann, R., Valentin, K., Weinberger, F., and Wiese, J., 2008, "The genus Laminaria sensu lato : recent insights and developments," European Journal of Phycology, 43(1), pp. 1-86.

ANNEX

Table 2. Overview over all clean nets. Mesh sizes and thread numbers are from the net manufacturer. Twine diameter and solidity are measured based on underwater images of nets stretched onto the measurement frame in the flow.

Net number	Mesh size [mm]	Thread number []	Twine diameter [mm]	Solidity [Sn]	Drag [N]	Stdev [N]	Stdev [% of drag]
N1	36	40	2.95	0.30	0.631	0.020	3,2
N2	40	36	2.85	0.25	0.601	0.013	2,2
N3	50	46	3.00	0.23	1.167	0.027	2,3
N4	32	32	2.60	0.29	0.685	0.021	3,1
N5	24	32	2.87	0.35	1.167	0.027	2,3
N6	40	24	2.27	0.20	0.488	0.014	2,9
N7	26	20	2.00	0.29	0.778	0.016	2,1
N8	8	8	1.08	0.54	1.876	0.059	3,1
N9	24	20	2.39	0.33	0.987	0.019	1,9
N10	15	10	1.31	0.35	1.107	0.03	2,7
N11	28	24	2.42	0.29	0.743	0.020	2,7
N12	18	12	1.43	0.32	1.016	0.022	2,2
N13	20	12	1.45	0.29	0.720	0.015	2,1
N14	30	24	2.51	0.27	0.705	0.015	2,1
N15	36	24	2.40	0.22	0.554	0.012	2,2
N16	26	16	2.05	0.30	0.799	0.017	2,1

Table 3.Overview over the amount and size of kelp on nets N3 and N4, the overall solidity of all kelp-fouled nets and the resulting drag in a flow of 0.1 ms^{-1}. Length is the average length of kelp blades, amount is the amount of kelp on the net, weight is the wet weight of all kelp on the net and solidity is the total solidity of kelp-fouled nets based on an analysis of underwater images of the nets in the flow with kelp being pressed against the net. Drag$_{with}$ is the drag when kelp was in the flow downstream from nets and Drag$_{against}$ is for kelp being pressed against the net on the upstream side.

Length [cm]	Amount []	Net number []	Weight [gm^{-2}]	Solidity [Sn]	Drag$_{against}$ [N]	Stdev [N]	Stdev [% of drag]	Drag$_{with}$ [N]	Stdev [N]	Stdev [% of drag]
10 - 15	3	N3	900	0.273	0.5093	0.0202	4,0		0.0366	
10 - 15	8	N3	950	0.387	0.9066	0.0213	2,3	0.3349	0.0230	46,1
10 - 15	15	N3	1000	0.327	1.0925	0.0192	1,8	0.4685	0.0176	3,8
10 - 15	25	N3	1045	0.471	1.4218	0.0364	2,6	0.5165	0.0317	6,1
20	3	N3	935	0.38	0.9643	0.0314	3,3	0.5757	0.0118	2,0
20	8	N3	1045	0.407				0.6805	0.0170	2,5
20	15	N3	1135	0.571	2.1585	0.0304	1,4	0.9859	0.0134	1,4
20	25	N3	1500	0.666	2.681	0.0381	1,4	0.7761	0.0280	3,6
30	3	N3	995	0.358	0.9547	0.0195	2,0	0.8893	0.0089	1,0
30	8	N3	1250	0.57	1.771	0.1056	6,0	0.6516	0.0101	1,6
30	15	N3	1920	0.594	2.1594	0.0275	1,3	1.0606	0.0141	1,3
30	25	N3	2270	0.634	2.3633	0.0345	1,5	1.2882	0.0153	1,2
10 - 15	3	N4	795	0.385	0.8843	0.0257	2,9	0.94	0.0173	1,8
10 - 15	8	N4	845	0.396	1.1753	0.0233	2,0	0.9107	0.0163	1,8

10 - 15	15	N4	845	0.394	1.1194	0.027	2,4	0.579	0.0258	4,5
10 - 15	25	N4	1050	0.608	1.9098	0.0386	2,0	1.1596	0.0183	1,6
20	3	N4	835	0.367	1.5444	0.0304	2,0	0.6405	0.0201	3,1
20	8	N4	960	0.449	1.1727	0.0212	1,8	1.1828	0.0137	1,2
20	15	N4	1170	0.566	2.0897	0.0294	1,4	0.9604	0.0334	3,5
20	25	N4	1305	0.807	3.4681	0.0431	1,2	1.5553	0.0192	1,2
30	3	N4	925	0.388	0.8069	0.0265	3,3	0.5831	0.0080	1,4
30	8	N4	1205	0.476	1.2766	0.0357	2,8	0.8486	0.0177	2,1
30	15	N4	2505	0.797	3.1336	0.0316	1,0	1.4868	0.0166	1,1
30	25	N4	2370	0.74	3.2747	0.0446	1,4	1.4749	0.0326	2,2

Table 4. Overview over the size and weight of blue mussels on nets N3 and N4, the overall solidity of all mussel-fouled nets and the resulting drag in a flow of 0.1 ms⁻¹. Size is the average shell length, weight is the wet weight of mussels on the net and solidity is the total solidity of mussel-fouled nets based on an analysis of underwater images of the fouled nets in the flow.

Mussel size [cm]	Net number	weight [gm⁻²]	Solidity [Sn]	Drag [N]	Stdev [N]	Stdev [% of drag]
0.5 - 1.6	N3	5580	0.774	2.5548	0.0511	2,0
2.5 - 4	N3	1585	0.351	1.151	0.0165	1,4
0.5 - 1.6	N3	1768	0.372	1.6314	0.0223	1,4
0.5 - 1.6	N3	2450	0.532	1.6737	0.0342	2,0
2.5 - 4	N4	2415	0.333	1.0636	0.0169	1,6
2.5 - 4	N4	2480	0.31	0.8331	0.0158	1,9
0.5 - 1.6	N4	4875	0.611	1.8295	0.025	1,4
0.5 - 1.6	N4	2520	0.393	1.336	0.0386	2,9
0.5 - 1.6	N4	1685	0.31	1.0942	0.0185	1,7

Estimation of the contribution of kelp attached to the upstream and downstream sides of nets to drag

The following example shows how much the positioning of seaweed on a net may influence net drag. Based on findings in Fig. 6 and Table 3 the drag on a clean net with an area of 0.2 m² and a solidity of about Sn = 0.3 experiences a drag of roughly 0.8 N in a flow of 0.1 ms⁻¹. Seaweed fouling on only the upstream side that causes the clean net solidity to double (fouled net solidity is 0.6) leads to a fouled net drag of 2.25 N in the same flow. Seaweed obstructing net openings so that the clean net solidity increases from Sn = 0.3 to a fouled net solidity of Sn = 0.6 leads to an increase of drag on the clean net with 180 % in a flow of 0.1 ms⁻¹. When the same amount of seaweed is attached to the downstream side, the drag on the net increases to 1.2 N in this flow, which is an increase by only 50 % of the clean net drag. When seaweed fouling is attached equally on both sides of the net and we assume no interaction of the flow around seaweed on the upstream and the downstream sides, the overall drag on the net would be about 3.45 N (drag on clean net with Sn = 0.3 is 0.8 N; additional drag due to fouling on the upstream side is 1.45 N; additional drag due to fouling on the downstream side is 0.4 N). That means that the additional drag due to fouling on the downstream side accounts for less than 15 % of the total drag on the fouled net, while the additional drag due to fouling on the upstream side accounts for over 40 % of the total drag. Of course, it is wrong to make the assumption of no interaction of the flow past seaweed on the upstream and the downstream side of the net, but an evaluation of the kelp distribution on nets in a flow together with data presented in Figure 6 and Table 3 can help to roughly estimate net drag based on net solidity calculated from underwater images. Choosing a shallow depth of field during the image capture can increase the likelihood of only including parts of kelps that are close to the net in the solidity calculations and a contribution of kelp on the downstream side of nets can be estimated using results shown in Figure 6b.